Journal of Magnetism and Magnetic Materials 344 (2013) 116–123

Contents lists available at SciVerse ScienceDirect

Journal of Magnetism and Magnetic Materials

journal homepage: www.elsevier.com/locate/jmmm

Aptamer conjugated paclitaxel and magnetic fluid loaded fluorescently tagged PLGA nanoparticles for targeted cancer therapy

Athulya Aravind, Remya Nair, Sreejith Raveendran, Srivani Veeranarayanan, Yutaka Nagaoka, Takahiro Fukuda, Takahashi Hasumura, Hisao Morimoto, Yasuhiko Yoshida, Toru Maekawa, D. Sakthi Kumar*

Bio Nano Electronics Research Center, Graduate School of Interdisciplinary New Science Toyo University Kawagoe, Saitama 350-8585, Japan

ARTICLE INFO

Article history:
Received 14 May 2012
Received in revised form
23 April 2013
Available online 5 June 2013

Keywords:
Nanodrug delivery
AS1411 aptamer
Paclitaxel
Magnetic fluid
PLGA Nanoparticles
Cancer therapy

ABSTRACT

Controlled and targeted drug delivery is an essential criterion in cancer therapy to reduce the side effects caused by non-specific drug release and toxicity. Targeted chemotherapy, sustained drug release and optical imaging have been achieved using a multifunctional nanocarrier constructed from poly (D, L-lactide-co-glycolide) nanoparticles (PLGA NPs), an anticancer drug paclitaxel (PTX), a fluorescent dye Nile red (NR), magnetic fluid (MF) and aptamers (Apt, AS1411, anti-nucleolin aptamer). The magnetic fluid and paclitaxel loaded fluorescently labeled PLGA NPs (MF-PTX-NR-PLGA NPs) were synthesized by a single-emulsion technique/solvent evaporation method using a chemical cross linker bis (sulfosuccinimidyl) suberate (BS3) to enable binding of aptamer on to the surface of the nanoparticles. Targeting aptamers were then introduced to the particles through the reaction with the cross linker to target the nucleolin receptors over expressed on the cancer cell surface. Specific binding and uptake of the aptamer conjugated magnetic fluid loaded fluorescently tagged PLGA NPs (Apt-MF-NR-PLGA NPs) to the target cancer cells induced by aptamers was observed using confocal microscopy. Cytotoxicity assay conducted in two cell lines (L929 and MCF-7) confirmed that targeted MCF-7 cancer cells were killed while control cells were unharmed. In addition, aptamer mediated delivery resulting in enhanced binding and uptake to the target cancer cells exhibited increased therapeutic effect of the drug. Moreover, these aptamer conjugated magnetic polymer vehicles apart from actively transporting drugs into specifically targeted tumor regions can also be used to induce hyperthermia or for facilitating magnetic guiding of particles to the tumor regions.

1. Introduction

Cancer treatment strategies are still dependent on the combination of conventional remedies such as radiation, chemotherapy, and surgical removal of tumors. The systemic toxicity and undesired side effects from conventional therapies have accelerated the progress in exploring site-specific therapies utilizing nanotechnology applications which will eliminate the tumors with limited effect on normal tissues [1,2]. Nanomedicine has the potential to increase the specificity of cancer therapy through the cancer cell-specific delivery of anticancer drugs using nanoparticles (NPs) equipped with targeting moieties [1,3]. Smart combinations of different nanoscale materials had led to the development of multifunctional nanoplatforms which can facilitate simultaneous cancer diagnosis and therapy [4].

Various studies have reported on the incorporation of magnetic resonance imaging (MRI) contrast agents and fluorescent dye simultaneously into biodegradable polymer nanomaterials for the construction of multimodal imaging probes [4–11]. A combination of MRI agent or optical imaging contrast agent and the chemotherapeutics loaded polymer nanoplatforms would be highly useful for simultaneous diagnostic and therapeutic applications [4,12–17]. These multifunctional polymer NPs can be functionalized with cancer specific ligands for simultaneous cancer-targeted MRI or optical imaging and magnetically guided drug delivery [4,10]. The magnetic guiding can enhance cancer targeting efficiency of the particles and can aid in delivering and accumulating the drug loaded particles at the desired place with the influence of an external magnetic field [4,18–20]. This can help to reduce the unwanted side effects and also to increase therapeutic efficacy of the drugs. Few studies have reported that chemotherapeutics bound magnetic carriers can be accumulated to the tumor sites

* Corresponding author. Tel.: +81 492 39 1636, +81 492 39 1640; fax: +81 492 34 2502.
E-mail addresses: sakthi@toyo.jp, drsakthi@gmail.com (D. Sakthi Kumar).

0304-8853/$ - see front matter © 2013 Elsevier B.V. All rights reserved.
http://dx.doi.org/10.1016/j.jmmm.2013.05.036

under the influence of an external magnetic field and this resulted in effective tumor regression [21–23]. It was also demonstrated that the amount of chemotherapeutic drug at the tumor areas increased due to the magnetic targeting compared to the normal systemic chemotherapy [24].

In our work we have prepared a multifunctional nanocarrier which efficiently combines cancer cell targeting with imaging, cargo (drug/dye) space, controlled release capabilities and tumor therapy. We have chosen FDA-approved poly (D, L-lactide-co-glycolide) (PLGA) polymers for developing our nanocarrier system. PLGA is having the property of diffusion and erosion-controlled drug release and furthermore this polymer is sensitive to pH and temperature-dependent degradation [25–28]. Paclitaxel (PTX), a broad spectrum anticancer drug, has been chosen for encapsulation to the polymer as the drug content [29–31]. Incorporation of super paramagnetic properties into NPs can aid in medical applications for hyperthermia therapy, magnetic manipulation and multimodal imaging [25,32–34]. Nile red dye (NR) was used to label the PLGA NPs [35]. Combination of fluorescent dye and magnetic fluid (MF) along with the chemotherapeutic PTX in the same NP enables bimodal imaging (by fluorescence and magnetic resonance, respectively) along with therapeutic feature [25]. For tumor targeting purpose, we have chosen a 26-nucleotide guanosine-rich (G-rich) DNA sequence (AS1411) which is believed to bind to the nucleolin receptors that is over expressed in the tumor cells compared to the normal cells [36,37]. Thus these multifunctional nanocarriers (Apt-MF-PTX-NR-PLGA NPs) can be targeted, guided and attracted to the cancer cells by two means—tumor specific aptamers and by applying an external magnetic field. Aptamers functionalized on the NPs play a vital role in targeting the particles to a specific subset of cells. Once the particles have been attached or internalized to the targeted areas, optical imaging is possible using the fluorescent dye incorporated within the particles. Upon confirming the exact particle localization, an external magnetic field can be applied at those particular sites to attract the remaining particles in circulation to the targeted location before they are subjected to renal clearance. Ultimately these actions can lead to increased accumulation of NPs in the tumor site and cellular uptake resulting in enhanced therapeutic efficiency. Moreover, these particles can be utilized for magnetic fluid hyperthermia (MFH) which is a kind of nanothermotherapy in therapeutic oncology. The superparamagnetic iron oxide particles in the PLGA NPs can generate heat upon exposure to alternative magnetic field (AMF) [38].

Our group had already reported on the removal of cancer cells by in vitro using clusters of aptamer conjugated magnetic NPs which is manipulated by external rotating magnetic fields [39]. Here we propose the multifunctional nanocarrier system [Scheme 1] comprising of (1) PTX for localized treatment, (2) NR fluorescent dye for tagging the PLGA NPs and optical imaging, (3) tumor-specific aptamers for cell targeting, and (4) superparamagnetic NPs for hyperthermia, magnetic guiding and imaging. Binding specificity and cellular uptake studies of the anti-nucleolin Apt-MF-NR-PLGA NPs were conducted in L929 cells and MCF-7 cells. A cell-based cytotoxicity assay was employed to verify successful entrapment and cytotoxic efficiency of the anticancer drug loaded within the NPs. Cell viability of normal fibroblast L929 cells and MCF-7 cancer cells is assessed in the presence of various nano formulations using the Alamar Blue assay. It was found that the MCF-7 cancer cells targeted with the aptamer conjugated polymer NPs were killed while the normal cells were unharmed. These multifunctional nanocarriers together with the tumor specific aptamers and external magnetic field can act synergistically to enhance the cancer targeting efficiency leading to the superior therapeutic efficiency.

2. Experimental details

The 50:50 PLGA(poly lactic-co-glycolic acid), MW 30–70 kDa with an inherent viscosity of 0.59 dL/g, polyvinyl alcohol (PVA), MW 12–23 kDa, 87–89% hydrolyzed, penicillin/streptomycin solution, N-hydroxysuccinimide (NHS), EDC (1-ethyl-3-(3-dimethylaminopropyl)-carbodiimide), bis(sulfosuccinimidyl) suberate (BS3) were obtained from Sigma-Aldrich. Ethyl acetate and all other reagents used were supplied by Fisher Scientific. Paclitaxel was obtained from Wako Chemicals. Ferrofluid containing magnetic nanoparticles of iron oxide coated with anionic surfactant was obtained from Ferrotec Coporation. Trypan blue, Nile red and Trypsin (0.25%) were purchased from Sigma Aldrich. Alamar blue stain was supplied by Invitrogen.

Aptamer AS1411 (NH2-5′-(GGTGGTGGTGGTTGTGGTGGTGGT-GG)-3′) was purchased from Operon.

2.1. Synthesis of MF-PTX-NR-PLGA NPs

The modified single-emulsion technique/solvent evaporation method was used to load magnetic fluids, fluorescent dye and anticancer drug into the polymer NPs [19,40,41]. Briefly, 65 mg of PLGA, 1 mg of paclitaxel and 10 μl of Nile red dye dissolved in 2 ml ethyl acetate was added to 2.2% aqueous solution of PVA containing 0.5 mg ml^{-1} of BS3 and 3 ml magnetic ferrofluid (MF) at two different concentrations (0.005 mg/ml and 50 mg/ml). This mixture was sonicated at room temperature using an ultrasonic processor system at 40% amplitude for 2 min in continuous mode. The excess solvent was evaporated by continuous stirring for 3 h followed by centrifugation to remove excess of aqueous solution. The separated NPs were washed in distill water three times.

2.2. Aptamer functionalization of MF-PTX-NR-PLGA NPs

Amine modified AS1411 aptamer was conjugated on to the carboxyl group of the NPs using the common conjugation strategy

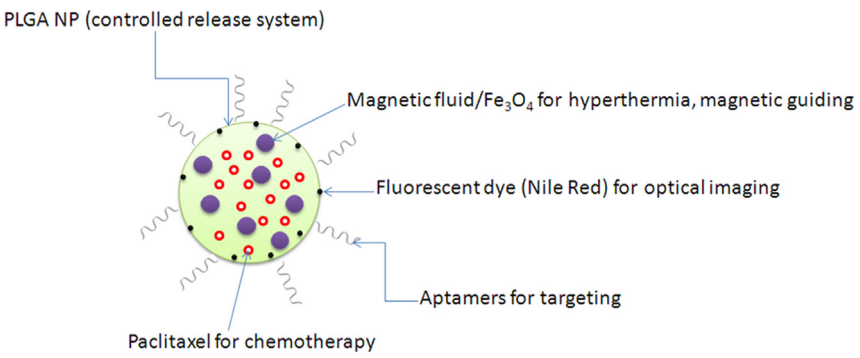

Scheme 1. Multifunctional nanocarrier

of carbodiimide chemistry [29]. The carboxyl groups on the NP surface was converted to succinimide by using 1-ethyl-3-[3–dimethylaminopropyl] carbodiimide hydrochloride (EDC) and N-hydroxysuccinimide (NHS), which was then allowed to react with NH_2-AS1411 aptamer. Briefly, a weighed quantity of the NPs was washed three times with 250 μL aliquots of a 10 mM PBS (pH 7.4) buffer and incubated with 200 μL of 400 mmol/L EDC and 200 μL of 100 mmol/L NHS for 15 min at room temperature with gentle shaking. The resulting NHS-activated particles are covalently linked to 10 μL aliquot of a 100 μM solution of amine-modified AS1411 aptamer. The sample was allowed to react for two hours with constant mixing at room temperature, and three final washes were performed using the 20 mM Tris–HCl, 5 mM $MgCl_2$ at pH 8.0. The resulting aptamer–NP bioconjugates were resuspended and preserved in suspension form in DNase RNase free water at 4 °C before use.

2.3. Particle characterization studies

The shape and surface morphology of NPs were studied using Field Emission Transmission Electron Micrograph, TEM (JEM-2200-FS), Atomic Force Microscope, AFM (Asylum Research) and Scanning Electron Microscope, SEM (JSEM 7400F). Dynamic light scattering analysis (Malvern Zetasizer Nano-ZS) was employed to analyze the size distribution and zeta potential of MF-PTX-NR-PLGA NPs in dispersion. X-ray photoelectron spectroscopy, XPS (AXIS His-165 Ultra, Kratos Analytical) was conducted to confirm the successful attachment of aptamers on to the NP surface. The samples were dropped onto a clean silicon substrate and dried before the experiment. The magnetization effect of MF-PTX-NR-PLGA NPs at low ferrofluid concentration and high ferrofluid concentrations were analyzed using Vibrating Sample Magnetometer, VSM (Lakeshore).

2.3.1. Drug encapsulation Studies

Initially a standard absorbance curve was established with a series of standard paclitaxel solution to facilitate the determination of the exact amount of drug within the nanoparticles (data not shown). Determination of the paclitaxel quantity within the nanoparticles was done by the UV–visible spectrophotometer at an absorbance of 227 nm. Based on this data, the drug incorporation efficiency was calculated for PTX-PLGA NPs and MF-PTX-PLGA NPs. Drug content and drug entrapment (%) is represented by Eqs. (1) and (2), respectively [35]

$$\text{Drug encapsulated} = \text{Drug total} - \text{Drugfiltrate} \quad (1)$$

$$\text{Drug encapsulation efficiency (\%)} = (\text{Amount of paclitaxel within the nanoparticles})/(\text{Amount of paclitaxel used in formation}) \times 100 \quad (2)$$

2.4. In vitro studies

Normal L929 mouse fibroblast cells and MCF-7 breast cancer cells obtained from Riken bioresource center, Japan were cultured in monolayers to 80% confluence using 25 cm^2 tissue culture flasks. The cultures were maintained in Dulbecco's minimal essential medium, (DMEM, Gibco) supplemented with 10% fetal bovine serum (FBS, Gibco) and 1% penicillin-streptomycin solution (Gibco) in a 5% CO_2-humidified atmosphere at 37 °C.

2.4.1. Binding efficiency and cellular uptake studies

Cellular uptake and targeting efficiency of MF-NR-PLGA NPs and Apt-MF-NR-PLGA NPs (particles prepared without anticancer drug) were studied in MCF-7 cells and L929 cells with the help of confocal microscopy. MCF-7 cells and L929 cells were seeded in glass based bottom well dish at a density of 1×10^4 cells/ml. The plates were incubated at 37 °C and grown to 70% confluency. Cells were treated with a fixed concentration, i.e.100 μg/ml, of MF-NR-PLGA NPs and Apt-MF-NR-PLGA NPs for 2 h. In our earlier work it was proved that 2 h incubation was quite sufficient for the internalization of polymer NPs inside live cells [29]. In addition, it was already reported that the aptamer-conjugated NPs were rapidly taken up by the cells due to the targeted binding and endocytosis which ultimately led to the higher level of NP internalization into cells within 2 h compared to the non-targeted particles [42]. At the end of the incubation period, the cell monolayers were rinsed three times with 1 ml of PBS buffer (0.01 M, 7.4) to remove excess NPs. MCF-7 plates treated with Apt-MF-NR-PLGA NPs were stained with Lysotracker to mark the location of lysosomes within the cells and to understand the localization of NPs within the cell. After staining, the cells were washed with PBS (0.01 M, PH 7.4) buffer to remove excess dye and the cells were viewed and imaged under a confocal laser scanning microscope.

2.4.2. Cytotoxicity assay

Cytotoxic assays like Alamar blue which is based on the cellular metabolic activity of cells were performed on normal as well as tumor cells to evaluate the cytotoxic potential of the NPs. Both the normal cells and tumor cells were treated with varying concentrations (250 μg/ml, 500 μg/ml and 1000 μg/ml) of magnetic fluid, MF-PLGA NPs, MF-PTX-PLGA NPs and Apt-MF-PTX-PLGA NPs for 5 days. Cells treated with only culturing media were used as respective controls. The media was changed on second and fourth days following the drug treatment; no further drug dose was added.

Alamar blue assay evaluates the proliferation and metabolic activity of cells. The mitochondrial reductase enzymes in living cells are active and reduce Alamar blue to form a different-colored product from the blue dye. This reducing ability of the cells accounts to the active metabolism taking place within the cells. When the samples are cytotoxic, the reducing ability of the cells decreases. The fluorescence intensity of Alamar blue assay was quantified at 580–610 nm. Based on this reading cell viability was calculated. All the experiments were repeated in triplicate and the viability of cells was determined on the fifth day of the treatment. Phase contrast studies were conducted to supplement the results of cytotoxic assay. The normal as well as tumor cells were cultured in 6 well plate with a density of approximately 50,000 cells per well and treated with the different nano formulations for 5 days and subjected to phase contrast microscopy.

3. Results and discussion

3.1. Particle characterization analysis

The surface morphology of MF and MF-PTX-NR-PLGA NPs was investigated using TEM. The TEM characterization of the magnetic fluid revealed a size about 10 nm [Fig. 1a]. The TEM [Fig. 1b] and AFM images [Fig. 2a & b] showed that MF-PTX-NR-PLGA NPs were spherical in shape. The surfaces of the particles were smooth and the size distribution ranged from 50 nm to 300 nm in diameter. Particle size distribution of the NPs was also studied using Zetasizer and the average particle size was noted to be 218 nm with zeta potential -27 ± 3 mv. Polydispersity index below 0.1 further indicated the dispersion stabilization of the nanoparticles.

The encapsulation efficiency of paclitaxel within PTX-PLGA NPs was found to be $40.44 \pm 4.5\%$. The drug concentration in MF-PTX-PLGA NPs varied from $36.12 \pm 3.5\%$ (low MF concentration) to $29 \pm 4.5\%$ (high MF concentration).

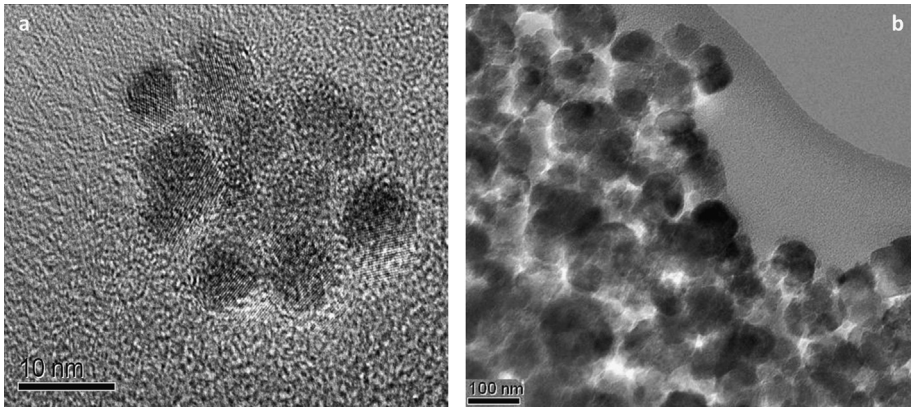

Fig. 1. TEM images of (a) Magnetic fluid and (b) MF-PTX-NR-PLGA NPs.

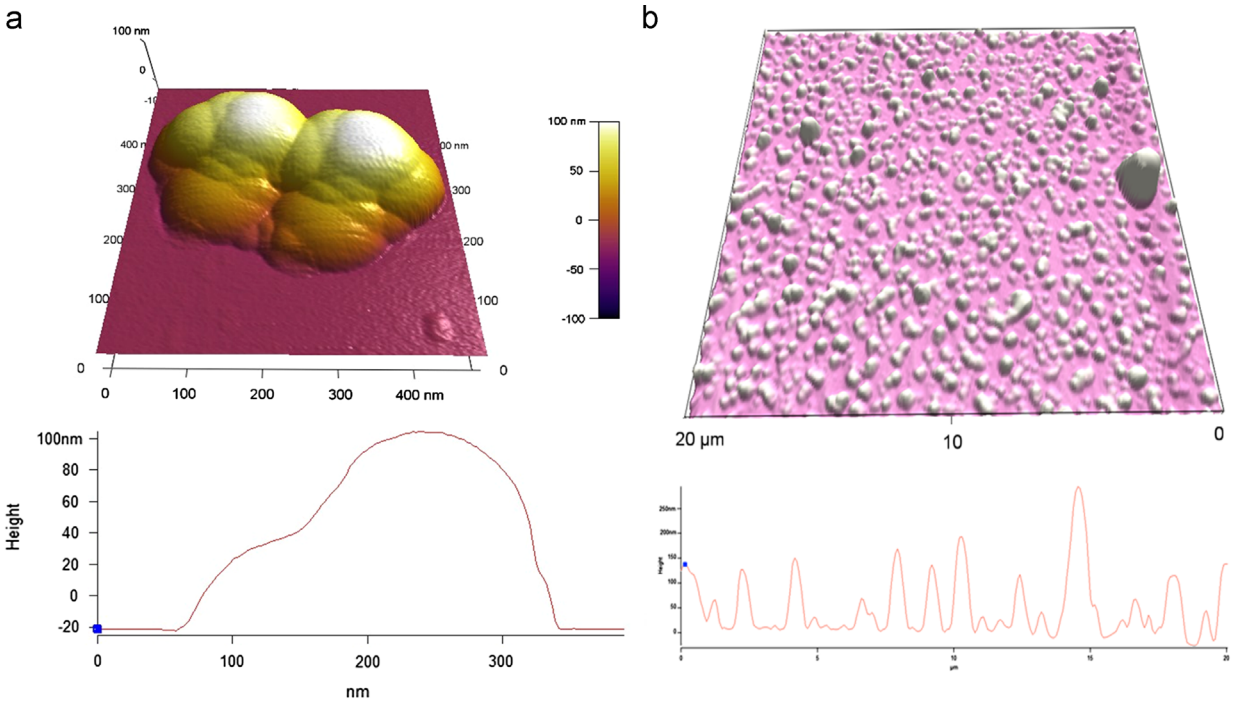

Fig. 2. (a & b): AFM image of MF-PTX-NR-PLGA NPs with their height images.

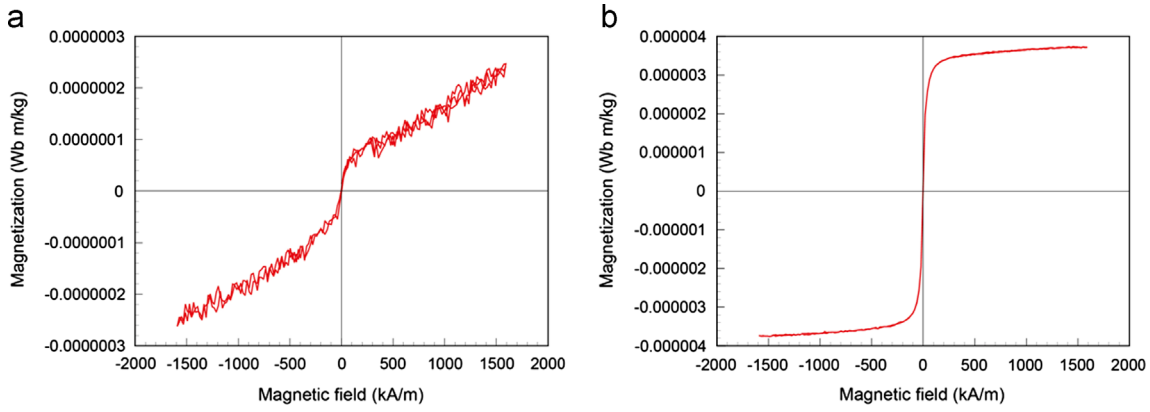

Fig. 3. Magnetization curves of (a) MF-PTX-NR-PLGA NPs at low concentration of magnetic fluids (Fe_3O_4—0.005 mg/ml) and (b) MF-PTX-NR-PLGA NPs at high concentration of magnetic fluids (Fe_3O_4—50 mg/ml).

The super paramagnetic behavior of the entrapped magnetic fluid in the PLGA core was confirmed by the magnetization studies using VSM. From the Fig. 3 it is evident that MF-PTX-NR-PLGA NPs exhibited super paramagnetic behavior at room temperature both at high and low concentrations of magnetic fluids. The saturation magnetization of MF-PTX-NR-PLGA NPs at low concentrations of magnetic fluids [Fig. 3a] is less compared to that of MF-PTX-NR-PLGA NPs with high concentrations of magnetic fluids [Fig. 3b] but they still show sufficient magnetization for their magnetic properties to be useful from the point of view of magnetic carrier technology.

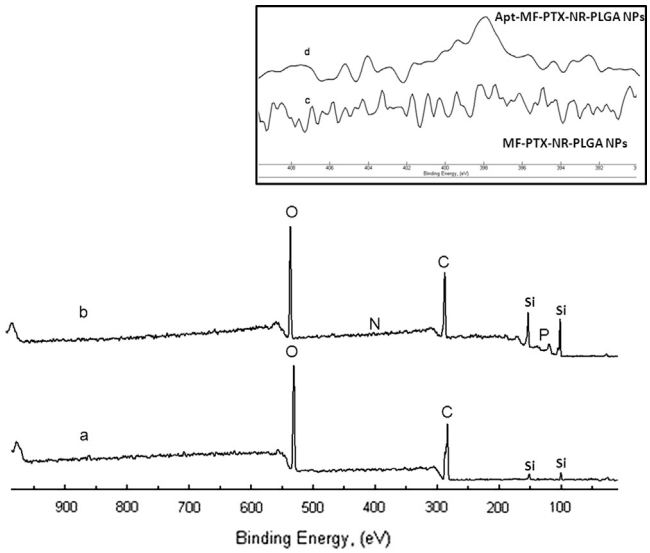

Fig. 4. X-ray photoelectron spectroscopy (XPS) peaks of the NPs. Wide scan spectra of the (a) MF-PTX-NR-PLGA NPs and (b) Apt-MF-PTX-NR-PLGA NPs. Inset contains the nitrogen spectra of the NPs. N1s signal spectra of (c) MF-PTX-NR-PLGA NPs and (d) Apt-MF-PTX-NR-PLGA NPs.

The surface elemental compositions of MF-PTX-NR-PLGA NPs and Apt-MF-PTX-NR-PLGA NPs were identified by X-ray Photoelectron spectroscopy. By utilizing XPS instrumentation, we also confirmed the coupling of aptamer onto the NP surfaces. The wide spectrum of MF-PTX-NR-PLGA NPs showed mainly carbon peak at 284 eV and oxygen peak at 532 eV [Fig. 4a]. The peaks at 99 eV and 152 eV are due to the photoelectrons from the silicon substrate used in the XPS experiment. This analysis support the fact that the drug as well magnetic fluids is loaded within the NP as the N peak which is the characteristic element of paclitaxel and Fe peak, characteristic of magnetic fluids are absent in the wide spectra of MF-PTX-NR-PLGA NPs. The VSM data has already shown that MF has been included within the NPs. Therefore the absence of Fe peak and N peak clearly suggests that MF as well as paclitaxel has been fully internalized within the core of the NPs.

In the case of Apt-MF-PTX-NR-PLGA NPs wide spectra, in addition to the carbon and oxygen peak we observed a small nitrogen peak at 398 eV [shown in the inset of Fig. 4] and phosphorus peak (131 eV) [Fig. 4b]. Since the presence of nitrogen and phosphorous among the chemical composition of the samples could only be credited to the aptamer and the aptamer conjugation bond, it was confirmed that the NPs surfaces were successfully decorated with aptamers which aid in targeted drug delivery. The N peak of MF-PTX-NR-PLGA NPs and Apt-MF-PTX-NR-PLGA NPs are shown in inset of Fig. 4c & d, respectively.

To confirm the embedding of magnetic fluid within the PLGA core we also performed Point SEM-EDS at different time intervals. The initial EDS data suggests that the smooth surface of the NPs were devoid of Fe [Fig. 5a]. Later, the electron beam exposure caused the etching of the polymer NP surface leading to the presence of a small Fe peak in the EDS analysis. The Fe peak became sharper upon increasing the surface etching by electron

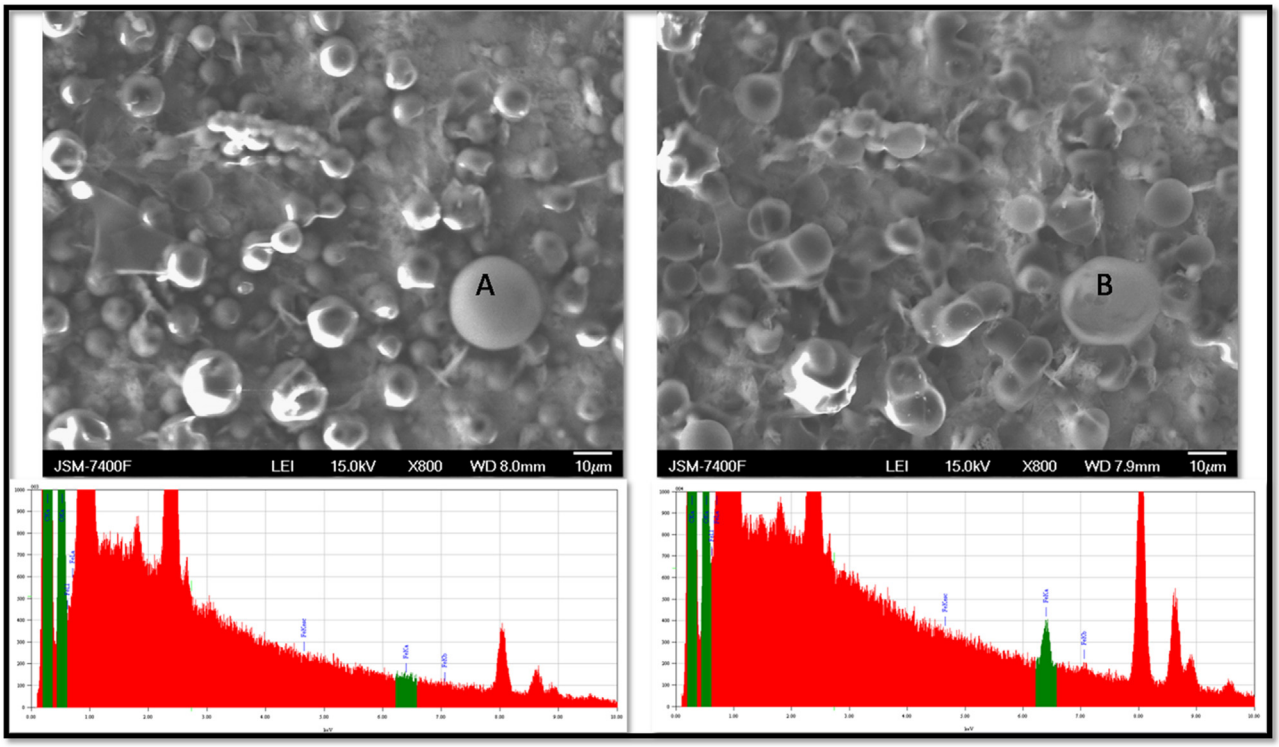

Fig. 5. Point SEM-EDS of MF-PTX-NR-PLGA NPs. (A) The immediate exposure of particles to electron beam showed that the particle surface to be smooth and spherical. No Fe peak was detected in the EDS spectra. (B) Prolonging the exposure of electron beam for few minutes resulted in the surface etching of the particles. The point EDS spectra at this stage gave a Fe peak which clearly indicated the entrapment of magnetic fluids inside the particles.

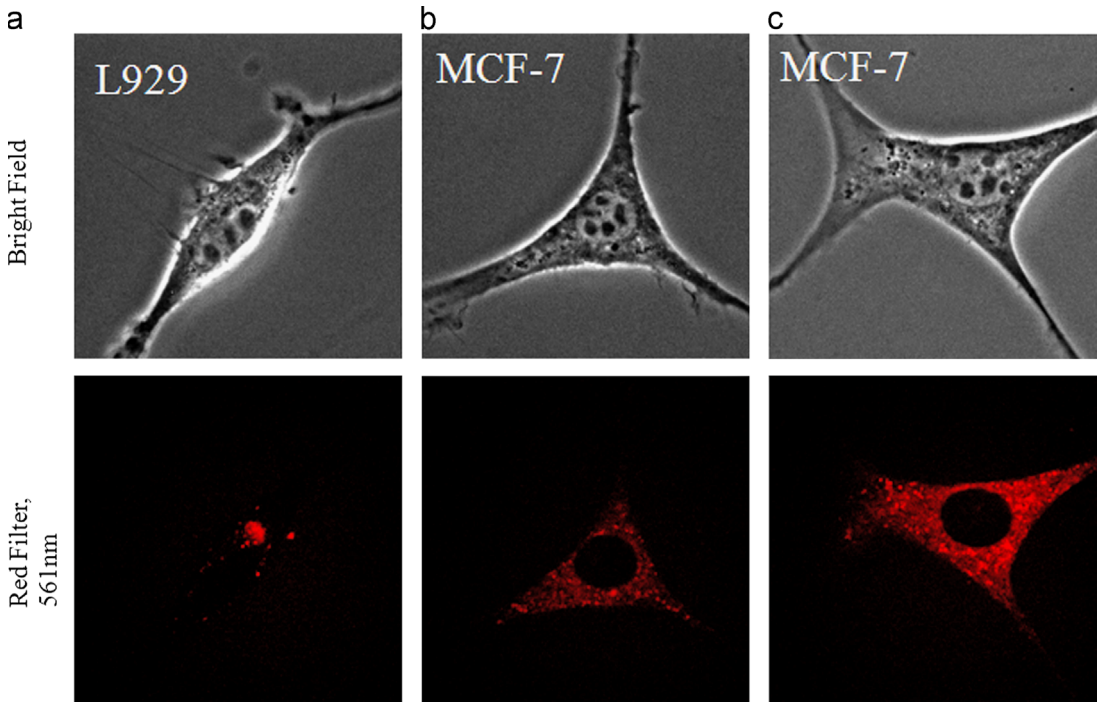

Fig. 6. Confocal microscopy images showing: (a) uptake of Apt-MF-NR-PLGA NPs in L929 cells (a normal cell line); (b) uptake of MF-NR-PLGA NPs (non-targeted NPs) by MCF-7 cells; (c) uptake of Apt-MF-NR-PLGA NPs (targeted NPs) by MCF-7 cells (tumor cell line). For each condition, particles were incubated with cells for 2 h. (Magnification 100 ×).

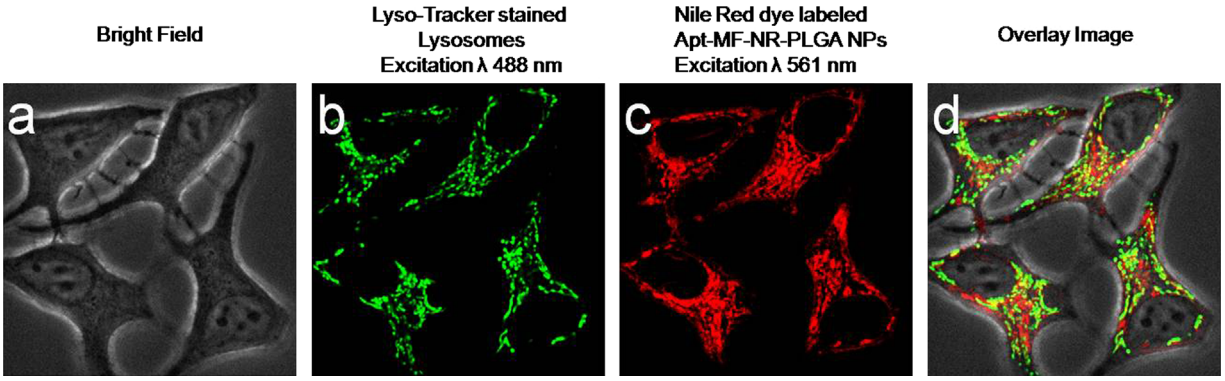

Fig. 7. Confocal laser scanning microscopy images show the internalization of aptamer conjugated magnetic-fluorescent PLGA NPs in cells (2 h incubation). (a) Bright field images of MCF-7 cells. (b) Green filters at excitation wavelength of 488 nm shows the green fluorescence from the Lysotracker dye which was used to stain the lysosomes. (c) Red filters at excitation wavelength 561 nm shows the red fluorescence from Apt-MF-NR-PLGA NPs. (d) Overlay of the bright field, green filter and red filter images. (Magnification 100 ×). (For interpretation of the references to color in this figure legend, the reader is referred to the web version of this article).

irradiation [Fig. 5b]. Thus we can conclude that the magnetic fluids are loaded within the particles and not present on the surface of the NPs.

3.2. *In vitro studies*

Cytoplasmic nucleolin is found to be present in tumor cells at elevated levels compared to the normal cells [37]. We have conjugated anti-nucleolin aptamers to the MF-NR-PLGA NPs (without paclitaxel drug) for binding specificity and uptake studies. A representative diagram for confocal imaging is shown in Fig. 6. Any detectable internalization of Apt-MF-NR-PLGA NPs in L929 cells (normal cells) was not observed after the incubation [Fig. 6a]. However, the uptake of the targeted NPs (Apt-MF-NR-PLGA NPs) was observed to be more than the non-targeted NPs (MF-NR-PLGA NPs) in MCF-7 cells (tumor cells) during the same period of time interval [Fig. 6b & c]. We also confirmed the cellular localization of particles within the lysosomes by staining the cells with Lysotracker which marks the lysosomes within the cell [Fig. 7]. Thus, it was proved that the targeted NPs have a tremendous potential for site-specific delivery and the detection of various cancer cell lines by incorporating appropriate targeting moiety on the surface.

The in vitro differential cytotoxicity of MF, MF-PLGA NPs, MF-PTX-PLGA NPs and Apt-MF-PTX-PLGA NPs were investigated in L929 cells and MCF-7 cells using Alamar Blue assay. The cells were treated with three different concentrations (250 μg/ml, 500 μg/ml and 1000 μg/ml) of the NP formulations for 5 days in triplicate. As shown in Fig. 8a & b, any acute cytotoxic effect was not observed when the cells were treated with MF moreover the MF-PLGA NPs were found to be highly biocompatible in nature. The targeted drug loaded particles were found to spare the normal cells while they killed about 85% of the tumor cells within 5 days [Fig. 8a & b]. The non-specific uptake and toxicity of the MF-PTX-PLGA NPs in the normal cells is due to their surface properties. This issue can be resolved by labeling the particles with a proper

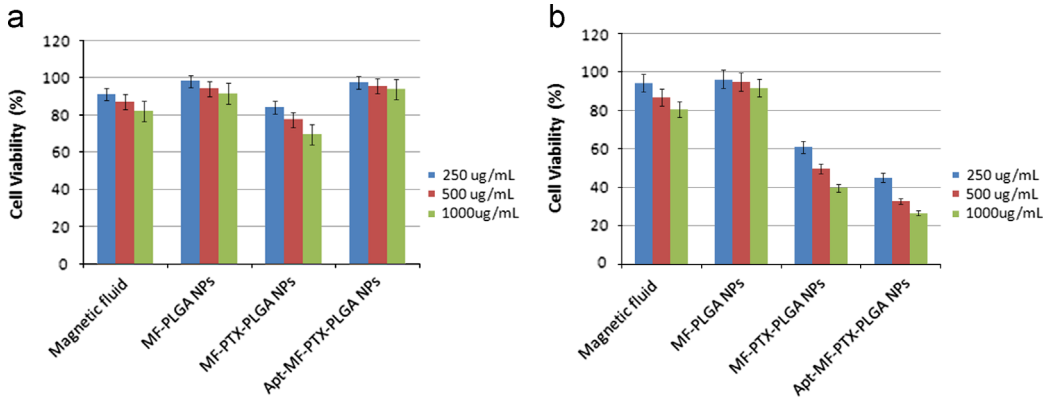

Fig. 8. (a) Cytotoxicity of magnetic fluid, MF-PLGA NPs, MF-PTX-PLGA NPS and Apt-MF-PTX-PLGA NPs on normal, L929 cell lines. (b) Cytotoxicity of magnetic fluid, MF-PLGA NPs, MF-PTX-PLGA NPs and Apt-MF-PTX-PLGA NPs cancer MCF7 cell lines.

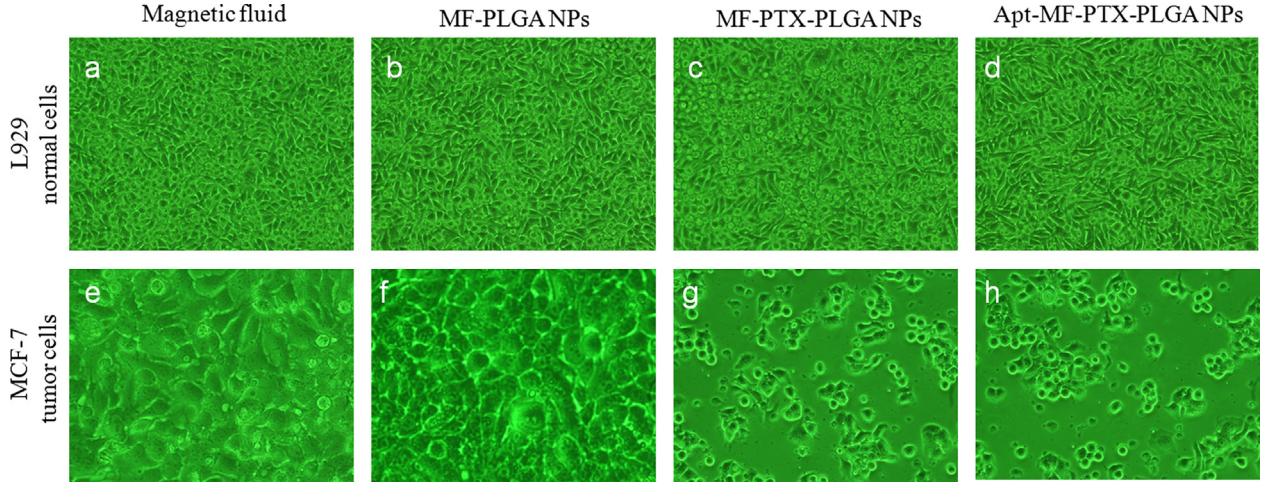

Fig. 9. Phase contrast images of L929 cells and MCF-7 cells after treating the cells with different NP formulations. (Magnification: 10 ×).

targeting ligand [Fig. 8a]. The results also demonstrated that the Apt-MF-PTX-PLGA NPs showed higher rate of cytotoxicity in tumor cells than non targeted MF-PTX-PLGA NPs [Fig. 8b].Thus we can conclude that the targeting ligand plays a prominent role in delivering the cargo to the selected subset of cells.

Additionally, the effects of all the nano formulations used for cytotoxicity assay were explored in detail with the help of phase contrast microscopy. Normal and cancer cell lines were cultured in 6 well plates with a density of approximately 50,000 cells per well and treated with different nano formulations at a concentration of 500 μg/ml for 5 days. The media was changed on the second and fourth day and no new doses of particles were added. After 5 days treatment, the cells were observed under phase contrast microscope. The cells treated with magnetic fluid and MF-PLGA NPs were active to a great extent; only a small percentage of cell death was noted in both cells [Fig. 9 a–b and e–f]. In the case of MF-PTX-PLGA NPs treated cells, both the normal L929 cells as well as MCF-7 cells were affected due to the drug release from the particles which are passively uptaken by the cells during the incubation time [Fig. 9c & g]. However, Apt-MF-PTX-PLGA NPs did not pose any serious intrinsic toxicity to the normal L929 cells [Fig. 9d]; the cells being viable and healthy, while these particles destroyed a major percentage of the MCF-7 cells plated [Fig. 9h]. This result directly supports the in vitro cytotoxicity assay.

The magnetization effect of the cell internalized particles was investigated using VSM. MCF-7 cells treated with Apt-MF-PTX-NR-PLGA NPs [Fig. 10] exhibited super paramagnetism to an extent. This result confirms the credibility of these targeted particles for further therapeutic and imaging applications such as magnetic guiding mediated drug delivery, hyperthermia and MRI imaging.

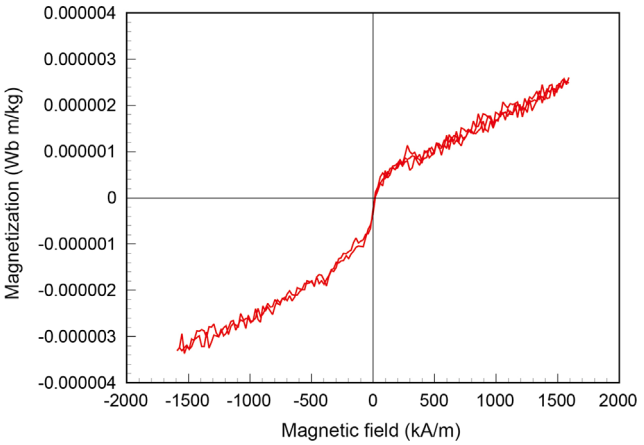

Fig. 10. VSM analysis of Apt-MF-PTX-NR-PLGA NPs treated MCF-7 cancer cells.

4. Conclusion

Our work reports on the synthesis, characterization and in vitro applications of tumor specific aptamer conjugated anticancer drug, fluorescent dye and magnetic fluid embedded PLGA NPs.

The aptamer conjugation on the particles have enabled enhanced cellular uptake into the targeted cells and have disabled the undesired toxicity in non-targeted cells. The improved specificity and internalization of these multifunctional nanocarriers and its rapid release of anticancer drug inside cancer cell lysosomes greatly facilitate the treatment of cancer with minimized systemic toxicity. In addition, these multifunctional NPs which were both magnetic fields responsive and useful as drug delivery systems were synthesized in a reproducible and simple way. Moreover, these multifunctional NPs can be exploited for various applications since it combine several perspectives like targeted drug delivery, hyperthermia therapy and MRI imaging in a single platform.

Acknowledgment

Athulya Aravind and Sreejith Raveendran thanks the Ministry of Education, Culture, Sports, Science and Technology (MEXT), Japan for the financial support given as Monbukagakusho fellowship. Also, part of this study has been supported by a Grant for the Programme of the Strategic Research Foundation at Private Universities S1101017, organized by the MEXT, Japan, since April 2012.

References

[1] T. Chen, M.I. Shukoor, R. Wang, et al., Smart multifunctional nanostructure for targeted cancer chemotherapy and magnetic resonance imaging, ACS Nano 5 (2011) 7866–7873.
[2] G. Poste, R. Kirsh, Site-specific (targeted) drug delivery in cancer therapy, Nature Biotechnology 1 (1983) 869–878.
[3] O.-M. Koo, I. Rubinstein, H. Onyuksel, Role of nanotechnology in targeted drug delivery and imaging: a concise review, Nanomedicine: Nanotechnology, Biology and Medicine 1 (2005) 193–212.
[4] J. Kim, J.E. Lee, S. Lee, et al., Designed fabrication of a multifunctional polymer nanomedical platform for simultaneous cancer-targeted imaging and magnetically guided drug delivery, Advanced Materials 20 (2008) 478–483.
[5] S. Santra, R.P. Bagwe, D. Dutta, et al., Synthesis and characterization of fluorescent, radio-opaque, and paramagnetic silica nanoparticles for multimodal bioimaging applications, Advanced Materials 17 (2005) 2165–2169.
[6] J.S. Kim, W.J. Rieter, K.M.L. Taylor, et al., Self-assembled hybrid nanoparticles for cancer-specific multimodal imaging, Journal of the American Chemical Society 129 (2007) 8962–8963.
[7] W.J. Rieter, J.S. Kim, K.M.L. Taylor, et al., Hybrid silica nanoparticles for multimodal imaging, Angewandte Chemie International Edition 46 (2007) 3680–3682.
[8] W.J. Rieter, K.M.L. Taylor, H. An, et al., Nanoscale metal–organic frameworks as potential multimodal contrast enhancing agents, Journal of the American Chemical Society 128 (2006) 9024–9025.
[9] J.-L. Bridot, A.-C. Faure, S. Laurent, et al., Hybrid gadolinium oxide nanoparticles: multimodal contrast agents for in vivo imaging, Journal of the American Chemical Society 129 (2007) 5076–5084.
[10] Z. Liu, P. Koczera, D. Doleschel, et al., Versatile synthetic strategies for PBCA-based hybrid fluorescent microbubbles and their potential theranostic applications to cell labelling and imaging, Chemical Communications (2012), http://dx.doi.org/10.1039/c2cc18048k.
[11] Y. Wang, Y.W. Ng, Y. Chen, et al., Formulation of superparamagnetic iron oxides by nanoparticles of biodegradable polymers for magnetic resonance imaging, Advanced Functional Materials 18 (2008) 308–318.
[12] J. Kim, S. Park, J.E. Lee, et al., Designed fabrication of multifunctional magnetic gold nanoshells and their application to magnetic resonance imaging and photothermal therapy, Angewandte Chemie International Edition 45 (2006) 7754–7758.
[13] S. Kim, T.Y. Ohul-Chanskyy, H.E. Pudavar, et al., Organically modified silica nanoparticles co-encapsulating photosensitizing drug and aggregation-enhanced two-photon absorbing fluorescent dye aggregates for two-photon photodynamic therapy, Journal of the American Chemical Society 129 (2007) 2669–2675.
[14] Z. Medarova, W. Pham, C. Farrar, et al., In vivo imaging of siRNA delivery and silencing in tumors, Nature Medicine 13 (2007) 372–377.
[15] N. Nasongkla, E. Bey, J. Ren, et al., Multifunctional polymeric micelles as cancer-targeted, MRI-ultrasensitive drug delivery systems, Nano Letters 6 (2006) 2427–2430.
[16] A.S. Lubbe, C. Bergemann, H. Riess, et al., Clinical experiences with magnetic drug targeting: a phase I study with 4′-epidoxorubicin in 14 patients with advanced solid tumors, Cancer Research 56 (1996) 4686–4693.
[17] S. Acharya, S.K. Sahoo, PLGA nanoparticles containing various anticancer agents and tumour delivery by EPR effect, Advanced Drug Delivery Reviews 63 (2011) 170–183.
[18] A. Juríková, K. Csach, M. Koneracká, et al., Magnetic polymer nanospheres for anticancer drug targeting, Journal of Physics: Conference Series 200 (2010) 122004.
[19] M. Koneracká, M. Múčková, V. Závišová, et al., Encapsulation of anticancer drug and magnetic particles in biodegradable polymer nanospheres, Journal of Physics 20 (2008) 204151.
[20] A.K.A. Silva, E.L. Silva, A.S. Carrico, et al., Magnetic carriers: a promising device for targeting drugs into the human body, Current Pharmaceutical Design 13 (2007) 1179–1185.
[21] A.S. Lübbe, C. Bergemann, W. Huhnt, et al., Preclinical experiences with magnetic drug targeting: tolerance and efficacy, Cancer Research 56 (1996) 4694–4701.
[22] C. Alexiou, W. Arnold, R.J. Klein, et al., Locoregional cancer treatment with magnetic drug targeting, Cancer Research 60 (2000) 6641–6648.
[23] M.W. Wilson, R.K. Kerlan, N.A. Fidelman, et al., Hepatocellular carcinoma: regional therapy with a magnetic targeted carrier bound to doxorubicin in a dual mr imaging/conventional angiography suite—initial experience with four patients, Radiology 230 (2004) 287–293.
[24] C. Alexiou, R. Jurgons, R. Schmid, et al., In vitro and in vivo investigations of targeted chemotherapy with magnetic nanoparticles, Journal of Magnetism and Magnetic Materials 293 (2005) 389–393.
[25] H.S. Cho, Z. Dong, G.M. Pauletti, et al., Fluorescent, superparamagnetic nanospheres for drug storage, targeting, and imaging: a multifunctional nanocarrier system for cancer diagnosis and treatment, ACS Nano 4 (2010) 5398–5404.
[26] M. Dunne, O.I. Corrigan, Z. Ramtoola, Influence of particle size and dissolution conditions on the degradation properties of polylactide-co-glycolide particles, Biomaterials 21 (2000) 1659–1668.
[27] A.C.R. Grayson, M.J. Cima, R. Langer, Size and temperature effects on poly (lactic-co-glycolic acid) degradation and microreservoir device performance, Biomaterials 26 (2005) 2137–2145.
[28] A.M. Reed, D.K. Gilding, Biodegradable polymers for use in surgery-poly (glycolic)/poly(lactic acid) homo and copolymers: 2. In vitro degradation, Polymer 22 (1981) 494–498.
[29] A. Aravind, S.H.Varghese, S. Veeranarayanan, et al.,Aptamer-labeled PLGA nanoparticles for targeting cancer cells. Cancer Nanotechnology. (2012) 10.1007/s12645-011-0024-6.
[30] J.M. Koziara, P.R. Lockman, D.D. Allen, et al., Paclitaxel nanoparticles for the potential treatment of brain tumors, Journal of Controlled Release 99 (2004) 259–269.
[31] H.-F. Liang, C.-T. Chen, S.-C Chen, et al., Paclitaxel-loaded poly(Lglutamic acid)-poly(lactide) nanoparticles as a targeted drug delivery system for the treatment of liver cancer, Biomaterials 27 (2006) 2051–2059.
[32] A. Jordan, R. Scholz, P. Wust, et al., Magnetic fluid hyperthermia (MFH): cancer treatment with Ac magnetic field induced excitation of biocompatible superparamagnetic nanoparticlesJournal of Magnetism and Magnetic Materials 201 (1999) 413–419.
[33] R. Hergt, S. Dutz, R. Muller, et al., Magnetic particle hyperthermia: nanoparticle magnetism and materials development for cancer therapy, Journal of Physics: Condensed Matter 18 (2006) 2919.
[34] T. Neuberger, B. Schopf, H. Hofmann, et al., Superparamagnetic nanoparticles for biomedical applications: possibilities and limitations of a new drug delivery system, Journal of Magnetism and Magnetic Materials 293 (2005) 483–496.
[35] A. Mukerjee, J.K. Vishwanatha, Formulation, characterization and evaluation of curcumin-loaded PLGA nanospheres for cancer therapy, Anticancer Research 29 (2009) 3867–3875.
[36] P.J. Bates, D.A Laber, Discovery and development of the G-rich oligonucleotide AS1411 as a novel treatment for cancer, Experimental and Molecular Pathology 86 (2009) 151–164.
[37] S. Soundararajan, L. Wang, V. Sridharan, et al., Plasma membrane nucleolin is a receptor for the anticancer aptamer AS1411 in MV4-11 leukemia cells, Leukemia and Lymphoma 76 (2009) 984–991.
[38] L. Zhao, Y. Wang, B. Yang, et al., Magnetic nanocomposite devices for cancer thermochemotherapy, in: Boreddy Reddy (Ed.), Advances in Nanocomposites-Synthesis, Characterization and Industrial Applications, InTech Publishers, 2011, ISBN: 978-953-307-165-7, http://dx.doi.org/10.5772/15344. Available from: 〈http://www.intechopen.com/books/advances-in-nanocomposites-synthesis-characterization-and-industrial-applications/magnetic-nanocomposite-devices-for-cancer-thermochemotherapy〉.
[39] B.G. Nair, Y. Nagaoka, H. Morimoto, et al., Aptamer conjugated magnetic nanoparticles as nanosurgeons, Nanotechnology 21 (2010) 455102.
[40] M.S. Cartiera, E.C. Ferreira, C. Caputo, et al., Partial correction of cystic fibrosis defects with PLGA nanoparticles encapsulating curcumin, Molecular Pharmaceutics 276 (2010) 675.
[41] S.I. Thamake, S.L. Raut, P. Ranjan, et al., Surface functionalization of PLGA nanoparticles by non-covalent insertion of a homo-bifunctional spacer for active targeting in cancer therapy, Nanotechnology 22 (2011) 035101.
[42] L. Zhang, J.M. Chan, F.X. Gu, et al., Self-assembled lipid–polymer hybrid nanoparticles: a robust drug delivery platform, ACS Nano 2 (2008) 1696–1702.